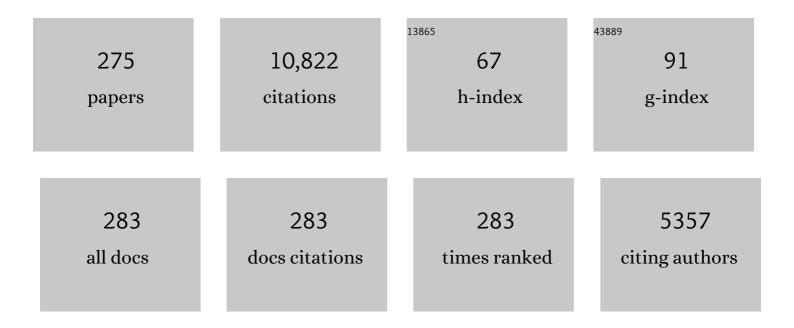
Boris B Straumal

List of Publications by Year in descending order

Source: https://exaly.com/author-pdf/287474/publications.pdf Version: 2024-02-01



#	Article	IF	CITATIONS
1	The Phase Transformations Induced by High-Pressure Torsion in Ti–Nb-Based Alloys. Microscopy and Microanalysis, 2022, 28, 946-952.	0.4	3
2	Modification of Biocorrosion and Cellular Response of Magnesium Alloy WE43 by Multiaxial Deformation. Metals, 2022, 12, 105.	2.3	1
3	Structure Refinement and Fragmentation of Precipitates under Severe Plastic Deformation: A Review. Materials, 2022, 15, 601.	2.9	20
4	Influence of faceting-roughening on triple-junction migration in zinc. International Journal of Materials Research, 2022, 96, 1147-1151.	0.3	1
5	Severe Plastic Deformation and Phase Transformations in High Entropy Alloys: A Review. Crystals, 2022, 12, 54.	2.2	13
6	Nanomaterials by severe plastic deformation: review of historical developments and recent advances. Materials Research Letters, 2022, 10, 163-256.	8.7	215
7	High Entropy Alloys Coatings Deposited by Laser Cladding: A Review of Grain Boundary Wetting Phenomena. Coatings, 2022, 12, 343.	2.6	20
8	Using Severe Plastic Deformation to Produce Nanostructured Materials with Superior Properties. Annual Review of Materials Research, 2022, 52, 357-382.	9.3	34
9	Grain boundary faceting close to the Σ3 coincidence misorientation in copper. International Journal of Materials Research, 2022, 95, 939-944.	0.3	0
10	Formation and Thermal Stability of the ï‰-Phase in Ti–Nb and Ti–Mo Alloys Subjected to HPT. Materials, 2022, 15, 4136.	2.9	2
11	Gradient bandgap narrowing in severely deformed ZnO nanoparticles. Materials Research Letters, 2021, 9, 58-64.	8.7	13
12	Wetting of grain boundary triple junctions by intermetallic delta-phase in the Cu–In alloys. Journal of Materials Science, 2021, 56, 7840-7848.	3.7	22
13	Omega Phase Formation in Ti–3wt.%Nb Alloy Induced by High-Pressure Torsion. Materials, 2021, 14, 2262.	2.9	6
14	Discontinuous Dissolution Reaction in a Fe-13.5 at. % Zn Alloy. Materials, 2021, 14, 1939.	2.9	2
15	The Enrichment of (Cu, Sn) Solid Solution Driven by High-Pressure Torsion. Crystals, 2021, 11, 766.	2.2	5
16	Phase Transformations in the AlMg Alloys Driven by Highâ€Pressure Torsion. Physica Status Solidi (B): Basic Research, 2021, 258, 2100210.	1.5	0
17	The formation of B2-precipitate and its effect on grain growth behavior in aluminum-containing CoCrNi medium-entropy alloy. Materials Letters, 2021, 303, 130481.	2.6	10
18	Formation of two amorphous phases in the Ni60Nb18Y22 alloy after high pressure torsion. Metallic Materials, 2021, 49, 17-22.	0.3	5

#	Article	IF	CITATIONS
19	The Grain Boundary Wetting Phenomena in the Ti-Containing High-Entropy Alloys: A Review. Metals, 2021, 11, 1881.	2.3	54
20	Grain Boundary Wetting Phenomena in High Entropy Alloys Containing Nitrides, Carbides, Borides, Silicides, and Hydrogen: A Review. Crystals, 2021, 11, 1540.	2.2	13
21	Grain Boundary Wetting by a Second Solid Phase in the High Entropy Alloys: A Review. Materials, 2021, 14, 7506.	2.9	23
22	Computer analysis of the cemented carbides' microstructure. Letters on Materials, 2021, 11, 447-451.	0.7	2
23	Cytotoxicity of biodegradable magnesium alloy WE43 to tumor cells in vitro: Bioresorbable implants with antitumor activity?. Journal of Biomedical Materials Research - Part B Applied Biomaterials, 2020, 108, 167-173.	3.4	24
24	Investigation on the precipitate formation and behavior in nitrogen-containing equiatomic CoCrFeMnNi high-entropy alloy. Materials Letters, 2020, 258, 126806.	2.6	16
25	Faceting of Twin Grain Boundaries in Highâ€Purity Copper Subjected to High Pressure Torsion. Advanced Engineering Materials, 2020, 22, 1900589.	3.5	4
26	Effect of internal stress on short-circuit diffusion in thin films and nanolaminates: Application to Cu/W nano-multilayers. Applied Surface Science, 2020, 508, 145254.	6.1	24
27	Stabilization of ultrafine-grained microstructure in high-purity copper by gas-filled pores produced by severe plastic deformation. Scripta Materialia, 2020, 178, 29-33.	5.2	11
28	Influence of β-Stabilizers on the α-Ti→ï‰-Ti Transformation in Ti-Based Alloys. Processes, 2020, 8, 1135.	2.8	7
29	Phase Transformations in Nd–Fe–B-Based Alloys under High Pressure Torsion at Different Temperatures. JETP Letters, 2020, 112, 37-44.	1.4	6
30	"Wetting―Phase Transitions by the Second Solid Phase for Linear Defects (Grain Boundary Triple) Tj ETQqO	0 0 rgBT / 1.4	Overlock 10
31	Bulk and Surface Low Temperature Phase Transitions in the Mg-Alloy EZ33A. Metals, 2020, 10, 1127.	2.3	44
32	The Effect of Equal-Channel Angular Pressing on Microstructure, Mechanical Properties, and Biodegradation Behavior of Magnesium Alloyed with Silver and Gadolinium. Crystals, 2020, 10, 918.	2.2	10
33	High pressure torsion of Cu–Ag and Cu–Sn alloys: Limits for solubility and dissolution. Acta Materialia, 2020, 195, 184-198.	7.9	24
34	Formation of the ω Phase in the Titanium—Iron System under Shear Deformation. JETP Letters, 2020, 111, 568-574.	1.4	65
35	Formation and Thermal Stability of ω-Ti(Fe) in α-Phase-Based Ti(Fe) Alloys. Metals, 2020, 10, 402.	2.3	12

36Thermal stability and microhardness of metastable ï‰-phase in the Ti-3.3Âat.% Co alloy subjected to high
pressure torsion. Journal of Alloys and Compounds, 2020, 834, 155132.5.57

#	Article	IF	CITATIONS
37	Grain boundaries in Nd-Fe-B-based alloys. Letters on Materials, 2020, 10, 566-571.	0.7	1
38	Competition for impurity atoms between defects and solid solution during high pressure torsion. Scripta Materialia, 2019, 173, 46-50.	5.2	32
39	Phase Transformations Induced by Severe Plastic Deformation. Materials Transactions, 2019, 60, 1489-1499.	1.2	63
40	Microstructure Evolution and Some Properties of Hard Magnetic FeCr30Co8 Alloy Subjected to Torsion Combined with Tension. Materials, 2019, 12, 3019.	2.9	3
41	Structural and Mechanical Properties of Ti–Co Alloys Treated by High Pressure Torsion. Materials, 2019, 12, 426.	2.9	22
42	Dissolution of Ag Precipitates in the Cu–8wt.%Ag Alloy Deformed by High Pressure Torsion. Materials, 2019, 12, 447.	2.9	15
43	Phase Transformations in Copper—Tin Solid Solutions at High-Pressure Torsion. JETP Letters, 2019, 110, 624-628.	1.4	9
44	The Effect of Equal-Channel Angular Pressing on the Microstructure, the Mechanical and Corrosion Properties and the Anti-Tumor Activity of Magnesium Alloyed with Silver. Materials, 2019, 12, 3832.	2.9	20
45	Thermal Stability of Athermal ωâ€īi(Fe) Produced upon Quenching of βâ€īi(Fe). Advanced Engineering Materials, 2019, 21, 1800158.	3.5	14
46	Effect of composition, annealing temperature, and high pressure torsion on structure and hardness of Ti–V and Ti–V–Al alloys. Journal of Applied Physics, 2019, 125, .	2.5	88
47	Grain Boundary Complexions and Phase Transformations in Al- and Cu-Based Alloys. Metals, 2019, 9, 10.	2.3	12
48	DIFFUSIVE AND DISPLACIVE PHASE TRANSFORMATIONS UNDER HIGH PRESSURE TORSION. Acta Metallurgica Slovaca, 2019, 25, 230-252.	0.7	4
49	Phase transitions in copper–silver alloys under high pressure torsion. International Journal of Materials Research, 2019, 110, 608-613.	0.3	8
50	Instabilities of interfaces between dissimilar metals induced by high pressure torsion. Materials Letters, 2018, 222, 172-175.	2.6	85
51	Diffusion in Materials Science and Technology. , 2018, , 261-275.		0
52	Transformation Pathway upon Heating of Ti–Fe Alloys Deformed by Highâ€Pressure Torsion. Advanced Engineering Materials, 2018, 20, 1700933.	3.5	23
53	Grain Boundary Wetting by a Second Solid Phase in Ti-Fe Alloys. Journal of Materials Engineering and Performance, 2018, 27, 4989-4992.	2.5	87
54	The α→ω and β→ω phase transformations in Ti–Fe alloys under high-pressure torsion. Acta Materialia, 20 337-351.	018, 144, 7.9	118

4

#	Article	IF	CITATIONS
55	Diffusive and displacive phase transitions in Ti–Fe and Ti–Co alloys under high pressure torsion. Journal of Alloys and Compounds, 2018, 735, 2281-2286.	5.5	35
56	Coarsening of (αTi) + (βTi) Microstructure in the Ti–Al–V Alloy at Constant Temperature. Advanced Engineering Materials, 2018, 20, 1800510.	3.5	23
57	Plastic flow and microstructural instabilities during high-pressure torsion of Cu/ZnO composites. Materials Characterization, 2018, 145, 389-401.	4.4	23
58	The α → ω Transformation in Titanium-Cobalt Alloys under High-Pressure Torsion. Metals, 2018, 8, 1.	2.3	281
59	Bulk Nanocrystalline Ferrite Stabilized through Grain Boundary Carbon Segregation. Advanced Engineering Materials, 2018, 20, 1800443.	3.5	37
60	Generation and healing of porosity in high purity copper by high-pressure torsion. Materials Characterization, 2018, 145, 1-9.	4.4	14
61	Contact angles of WC/WC grain boundaries with binder in cemented carbides with various carbon content. Materials Letters, 2017, 196, 1-3.	2.6	20
62	The effect of bismuth on microstructure evolution of ultrafine grained copper. Materials Letters, 2017, 199, 156-159.	2.6	9
63	Statistics of GB misorientations in 2D polycrystalline copper foil. Materials Letters, 2017, 196, 377-380.	2.6	5
64	Phase transitions in Cu-based alloys under high pressure torsion. Journal of Alloys and Compounds, 2017, 707, 20-26.	5.5	61
65	Pseudopartial wetting of W/W grain boundaries by the nickel-rich layers. Materials Letters, 2017, 192, 101-103.	2.6	22
66	High-pressure torsion driven phase transformations in Cu–Al–Ni shape memory alloys. Acta Materialia, 2017, 125, 274-285.	7.9	41
67	Competition between precipitation and dissolution in Cu–Ag alloys under high pressure torsion. Acta Materialia, 2017, 122, 60-71.	7.9	100
68	Grain boundary wetting transition in Alâ \in "Mg alloys. Materials Letters, 2017, 186, 82-85.	2.6	41
69	Grain Boundary Wetting in the Nd-Fe-B-Based Alloy. Defect and Diffusion Forum, 2017, 380, 173-180.	0.4	5
70	Ferromagnetic behaviour of ZnO: the role of grain boundaries. Beilstein Journal of Nanotechnology, 2016, 7, 1936-1947.	2.8	99
71	Grain boundary complexions and pseudopartial wetting. Current Opinion in Solid State and Materials Science, 2016, 20, 247-256.	11.5	99
72	Grain boundary wetting phase transitions in peritectic copper—cobalt alloys. Physics of the Solid State, 2016, 58, 742-746.	0.6	22

#	Article	IF	CITATIONS
73	Observation of Pseudopartial Grain Boundary Wetting in the NdFeB-Based Alloy. Journal of Materials Engineering and Performance, 2016, 25, 3303-3309.	2.5	35
74	Grain refinement of intermetallic compounds in the Cu–Sn system under high pressure torsion. Materials Letters, 2016, 179, 12-15.	2.6	20
75	Microstructure evolution and mechanical behavior of ultrafine Ti 6Al 4V during low-temperature superplastic deformation. Acta Materialia, 2016, 121, 152-163.	7.9	148
76	Formation regularities of grain-boundary interlayers of the α-Ti phase in binary titanium alloys. Russian Journal of Non-Ferrous Metals, 2016, 57, 229-235.	0.6	26
77	Effect of high pressure torsion on microstructure of Cu-Sn alloys with different content of Hume Rothery phase. Materials Characterization, 2016, 118, 411-416.	4.4	12
78	Growth of (αTi) grain-boundary layers in Ti–Co alloys. Russian Journal of Non-Ferrous Metals, 2016, 57, 703-709.	0.6	53
79	Preface to the special section on high-temperature capillarity. Journal of Materials Science, 2016, 51, 1669-1670.	3.7	0
80	How to Tune the Alumina Aerogels Structure by the Variation of a Supercritical Solvent. Evolution of the Structure During Heat Treatment. Journal of Physical Chemistry C, 2016, 120, 3319-3325.	3.1	22
81	Phase transformations in a Cu Cr alloy induced by high pressure torsion. Materials Characterization, 2016, 114, 151-156.	4.4	18
82	Review: grain boundary faceting–roughening phenomena. Journal of Materials Science, 2016, 51, 382-404.	3.7	97
83	Phase Transformations in Ti–Fe Alloys Induced by Highâ€Pressure Torsion. Advanced Engineering Materials, 2015, 17, 1835-1841.	3.5	95
84	Ultrafine Grained Structures Resulting from SPDâ€Induced Phase Transformation in Al–Zn Alloys. Advanced Engineering Materials, 2015, 17, 1821-1827.	3.5	86
85	Interfacial dominated ferromagnetism in nanograined ZnO: a μSR and DFT study. Scientific Reports, 2015, 5, 8871.	3.3	97
86	Severe Plastic Deformation on Powder Metallurgy Cu–Al–Ni Shape Memory Alloys. Materials Today: Proceedings, 2015, 2, S747-S750.	1.8	15
87	Wear-resistance and hardness: Are they directly related for nanostructured hard materials?. International Journal of Refractory Metals and Hard Materials, 2015, 49, 203-211.	3.8	62
88	Pseudopartial wetting of WC/WC grain boundaries in cemented carbides. Materials Letters, 2015, 147, 105-108.	2.6	51
89	Amorphization of Nd–Fe–B alloy under the action of high-pressure torsion. Materials Letters, 2015, 145, 63-66.	2.6	35
90	Direct observation of strain-induced non-equilibrium grain boundaries. Materials Letters, 2015, 159, 432-435.	2.6	9

#	Article	IF	CITATIONS
91	Influence of the grain boundary character on the temperature of transition to complete wetting in the Cu–In system. Journal of Materials Science, 2015, 50, 4762-4771.	3.7	32
92	Phase transitions induced by severe plastic deformation: steady-state and equifinality. International Journal of Materials Research, 2015, 106, 657-664.	0.3	76
93	Transformations of Cu(in) supersaturated solid solutions under high-pressure torsion. Materials Letters, 2015, 138, 255-258.	2.6	15
94	Pseudopartial wetting of grain boundaries in severely deformed Al-Zn alloys. Russian Journal of Non-Ferrous Metals, 2015, 56, 44-51.	0.6	42
95	Amorphization of crystalline phases in the Nd–Fe–B alloy driven by the high-pressure torsion. Materials Letters, 2015, 161, 735-739.	2.6	29
96	Microstructure evolution of Cu – 22 % In alloy subjected to the high pressure torsion. IOP Conference Series: Materials Science and Engineering, 2014, 63, 012093.	0.6	6
97	Transformation of Hume-Rothery phases under the action of high pressure torsion. JETP Letters, 2014, 100, 376-379.	1.4	16
98	Grain Boundary Phenomena in an Ultrafineâ€Grained Al–Zn Alloy with Improved Mechanical Behavior for Microâ€Devices. Advanced Engineering Materials, 2014, 16, 1000-1009.	3.5	92
99	Reversible "Wetting―of grain boundaries by the second solid phase in the Cu-In system. JETP Letters, 2014, 100, 535-539.	1.4	43
100	Phase transitions during high pressure torsion of Cu Co alloys. Materials Letters, 2014, 118, 111-114.	2.6	71
101	Phase transitions in metallic alloys driven by the high pressure torsion. Archives of Civil and Mechanical Engineering, 2014, 14, 242-249.	3.8	112
102	Continuous and Discontinuous αTi Layers Between Grains of β(Ti,Co) Phase. Journal of Materials Engineering and Performance, 2014, 23, 1580-1584.	2.5	6
103	Grain boundary films in Al–Zn alloys after high pressure torsion. Scripta Materialia, 2014, 70, 59-62.	5.2	110
104	Increase of Fe solubility in ZnO induced by the grain boundary adsorption. Journal of Materials Science, 2014, 49, 4490-4498.	3.7	77
105	Strengthening zones in the Co matrix of WC–Co cemented carbides. Scripta Materialia, 2014, 83, 17-20.	5.2	98
106	Grain boundary wetting and premelting in the Cu–Co alloys. Journal of Alloys and Compounds, 2014, 615, S183-S187.	5.5	17
107	Phase transformations in Al–Mg–Zn alloys during high pressure torsion and subsequent heating. Journal of Materials Science, 2013, 48, 4758-4765.	3.7	13
108	Ferromagnetism of zinc oxide nanograined films. JETP Letters, 2013, 97, 367-377.	1.4	109

#	Article	IF	CITATIONS
109	Interrelation of depletion and segregation in decomposition of nanoparticles. Philosophical Magazine, 2013, 93, 1677-1689.	1.6	6
110	SPD-induced changes of structure and magnetic properties in the Cu–Co alloys. Materials Letters, 2013, 98, 217-221.	2.6	15
111	Contribution of tilt boundaries to the total energy spectrum of grain boundaries in polycrystals. JETP Letters, 2013, 96, 582-587.	1.4	7
112	Grain boundaries as the controlling factor for the ferromagnetic behaviour of Co-doped ZnO. Philosophical Magazine, 2013, 93, 1371-1383.	1.6	100
113	Ferromagnetic behaviour of Fe-doped ZnO nanograined films. Beilstein Journal of Nanotechnology, 2013, 4, 361-369.	2.8	92
114	Effective Temperature of High Pressure Torsion in Zr-Nb Alloys. High Temperature Materials and Processes, 2012, 31, .	1.4	20
115	Accelerated Diffusion and Phase Transformations in Co–Cu Alloys Driven by the Severe Plastic Deformation. Materials Transactions, 2012, 53, 63-71.	1.2	117
116	Grain boundary wetting in the NdFeB-based hard magnetic alloys. Journal of Materials Science, 2012, 47, 8352-8359.	3.7	35
117	Apparently complete grain boundary wetting in Cu–In alloys. Journal of Materials Science, 2012, 47, 8336-8343.	3.7	43
118	Heat effect of grain boundary wetting in Al–Mg alloys. Journal of Materials Science, 2012, 47, 8367-8371.	3.7	18
119	Effect of the wetting of grain boundaries on the formation of a solid solution in the Al-Zn system. JETP Letters, 2012, 96, 380-384.	1.4	20
120	Ferromagnetism of nanostructured zinc oxide films. Physics of Metals and Metallography, 2012, 113, 1244-1256.	1.0	82
121	Wetting of grain boundaries in hard-magnetic Nd-Fe-B alloys. Russian Journal of Non-Ferrous Metals, 2012, 53, 450-456.	0.6	16
122	Complete and Incomplete Wetting of Ferrite Grain Boundaries by Austenite in the Low-Alloyed Ferritic Steel. Journal of Materials Engineering and Performance, 2012, 21, 667-670.	2.5	102
123	Grain Boundary Wetting by a Second Solid Phase in the Zr-Nb Alloys. Journal of Materials Engineering and Performance, 2012, 21, 721-724.	2.5	82
124	Amorphous interlayers between crystalline grains in ferromagnetic ZnO films. Materials Letters, 2012, 71, 21-24.	2.6	89
125	Phase transformations in the severely plastically deformed Zr–Nb alloys. Materials Letters, 2012, 81, 225-228.	2.6	61
126	Gradual softening of Al–Zn alloys during high-pressure torsion. Materials Letters, 2012, 84, 63-65.	2.6	90

#	Article	IF	CITATIONS
127	Strain rate sensitivity studies in an ultrafine-grained Al–30wt.% Zn alloy using micro- and nanoindentation. Materials Science & Engineering A: Structural Materials: Properties, Microstructure and Processing, 2012, 543, 117-120.	5.6	92
128	Deformation-driven formation of equilibrium phases in the Cu–Ni alloys. Journal of Materials Science, 2012, 47, 360-367.	3.7	63
129	Faceting–roughening of twin grain boundaries. Journal of Materials Science, 2012, 47, 1641-1646.	3.7	11
130	Amorphous grain boundary layers in the ferromagnetic nanograined ZnO films. Thin Solid Films, 2011, 520, 1192-1194.	1.8	86
131	Wetting transition of grain boundaries in the Sn-rich part of the Sn–Bi phase diagram. Journal of Materials Science, 2011, 46, 1557-1562.	3.7	18
132	First measurement of the heat effect of the grain boundary wetting phase transition. Journal of Materials Science, 2011, 46, 4243-4247.	3.7	15
133	Transmission electron microscopy investigation of boundaries between amorphous "grains―in Ni50Nb20Y30 alloy. Journal of Materials Science, 2011, 46, 4336-4342.	3.7	73
134	Inversed solid-phase grain boundary wetting in the Al–Zn system. Journal of Materials Science, 2011, 46, 4349-4353.	3.7	77
135	Influence of texture on the ferromagnetic properties of nanograined ZnO films. Physica Status Solidi (B): Basic Research, 2011, 248, 1581-1586.	1.5	81
136	Structure and Properties of Nanograined Fe–C Alloys after Severe Plastic Deformation. Advanced Engineering Materials, 2011, 13, 463-469.	3.5	74
137	Wetting Transition of Grain Boundaries in Tin–Rich Indium-Based Alloys and Its Influence on Electrical Properties. Materials Transactions, 2010, 51, 1677-1682.	1.2	11
138	Ferromagnetic properties of the Mn-doped nanograined ZnO films. Journal of Applied Physics, 2010, 108, .	2.5	108
139	Wetting of grain boundaries in Al by the solid Al3Mg2 phase. Journal of Materials Science, 2010, 45, 2057-2061.	3.7	87
140	Contact angles by the solid-phase grain boundary wetting (coverage) in the Co–Cu system. Journal of Materials Science, 2010, 45, 4271-4275.	3.7	76
141	Unusual super-ductility at room temperature in an ultrafine-grained aluminum alloy. Journal of Materials Science, 2010, 45, 4718-4724.	3.7	125
142	Grain boundary ridges and triple lines. Scripta Materialia, 2010, 62, 924-927.	5.2	11
143	Grain boundary layers in nanocrystalline ferromagnetic zinc oxide. JETP Letters, 2010, 92, 396-400.	1.4	87
144	Study on the Solidus Line in Sn-Rich Region of Sn-In Phase Diagram. Journal of Phase Equilibria and Diffusion, 2009, 30, 254-257.	1.4	12

#	Article	IF	CITATIONS
145	Fe–C nanograined alloys obtained by high-pressure torsion: Structure and magnetic properties. Materials Science & Engineering A: Structural Materials: Properties, Microstructure and Processing, 2009, 503, 185-189.	5.6	74
146	Increase of Mn solubility with decreasing grain size in ZnO. Journal of the European Ceramic Society, 2009, 29, 1963-1970.	5.7	142
147	Grain boundary faceting-roughening in Zn. Crystallography Reports, 2009, 54, 1070-1078.	0.6	3
148	Magnetization study of nanograined pure and Mn-doped ZnO films: Formation of a ferromagnetic grain-boundary foam. Physical Review B, 2009, 79, .	3.2	343
149	Effect of severe plastic deformation on the coercivity of Co–Cu alloys. Philosophical Magazine Letters, 2009, 89, 649-654.	1.2	18
150	Second-order faceting–roughening of the tilt grain boundary in zinc. International Journal of Materials Research, 2009, 100, 525-529.	0.3	6
151	Structure, phase composition, and microhardness of carbon steels after high-pressure torsion. Journal of Materials Science, 2008, 43, 3800-3805.	3.7	12
152	Motion of the faceted 57Ű \$\$ [11overline{2} 0] \$\$ tilt grain boundary in zinc. Journal of Materials Science, 2008, 43, 3860-3866.	3.7	9
153	Coercivity and domain structure of nanograined Fe–C alloys after high-pressure torsion. Journal of Materials Science, 2008, 43, 3775-3781.	3.7	8
154	Wetting transition of grain-boundary triple junctions. Acta Materialia, 2008, 56, 925-933.	7.9	85
155	Effect of faceting on grain boundary motion in Zn. Acta Materialia, 2008, 56, 2728-2734.	7.9	71
156	Thermal evolution and grain boundary phase transformations in severely deformed nanograined Al–Zn alloys. Acta Materialia, 2008, 56, 6123-6131.	7.9	89
157	Increase of Co solubility with decreasing grain size in ZnO. Acta Materialia, 2008, 56, 6246-6256.	7.9	125
158	Wetting and premelting of triple junctions and grain boundaries in the Al–Zn alloys. Materials Science & Engineering A: Structural Materials: Properties, Microstructure and Processing, 2008, 495, 126-131.	5.6	17
159	First observation of a wetting phase transition in low-angle grain boundaries. JETP Letters, 2008, 88, 537-542.	1.4	36
160	Hardmetals with nanograin reinforced binder: Binder fine structure and hardness. International Journal of Refractory Metals and Hard Materials, 2008, 26, 583-588.	3.8	30
161	Evaluation of the Coverage Pattern on the Fracture Surface of Bi-Embrittled Cu Grain Boundaries by Means of Auger Electron Spectroscopy. Defect and Diffusion Forum, 2008, 273-276, 643-648.	0.4	0
162	The Influence of Quenching Baths on Grain Boundary Wetting Transition in Sn–25 at% In alloy. Defect and Diffusion Forum, 2008, 273-276, 649-654.	0.4	0

#	Article	IF	CITATIONS
163	Non-destructive compositional analysis of historic organ reed pipes. Journal of Physics Condensed Matter, 2008, 20, 104250.	1.8	8
164	Continuous and discontinuous grain-boundary wetting in <mml:math xmlns:mml="http://www.w3.org/1998/Math/MathML" display="inline"><mml:mrow><mml:msub><mml:mrow><mml:mtext>Zn</mml:mtext></mml:mrow><mml:m Physical Review B, 2008, 78, .</mml:m </mml:msub></mml:mrow></mml:math 	i>x <td>><!--80/mml:msub</td--></td>	> 80/mml:msub</td
165	Reversible transformation of a grain-boundary facet into a rough-to-rough ridge in zinc. Philosophical Magazine Letters, 2008, 88, 27-36.	1.2	8
166	Distribution of impurities and minor components in nanostructured conducting oxides. International Journal of Nanomanufacturing, 2008, 2, 253.	0.3	16
167	Reconstruction of Historical Alloys for Pipe Organs Brings True Baroque Music Back to Life. MRS Bulletin, 2007, 32, 249-255.	3.5	8
168	Faceting of Σ3 Grain Boundaries in Al. Materials Science Forum, 2007, 558-559, 949-954.	0.3	7
169	Grain boundary phase observed in Al–5 at.% Zn alloy by using HREM. Philosophical Magazine Letters, 2007, 87, 423-430.	1.2	30
170	Hot isostatic pressing of Cu–Bi polycrystals with liquid-like grain boundary layers. Acta Materialia, 2007, 55, 335-343.	7.9	9
171	Structural changes in aluminum alloys upon severe plastic deformation. Physics of the Solid State, 2007, 49, 868-873.	0.6	22
172	The effect of bismuth segregation on the faceting of Σ3 and Σ9 coincidence boundaries in copper bicrystals. International Journal of Materials Research, 2007, 98, 451-456.	0.3	13
173	Temperature influence on the faceting of 3 and 9 grain boundaries in Cu. Acta Materialia, 2006, 54, 167-172.	7.9	80
174	Softening of nanostructured Al–Zn and Al–Mg alloys after severe plastic deformation. Acta Materialia, 2006, 54, 3933-3939.	7.9	161
175	Silicon carbide and diamond for high temperature device applications. Journal of Materials Science: Materials in Electronics, 2006, 17, 1-25.	2.2	227
176	Structure of Historical Brass Tongues and Shallots from Baroque Organs. Defect and Diffusion Forum, 2006, 249, 275-280.	0.4	9
177	Grain Boundary Wetting in Zn Bicrystals by a Sn-Based Melt. Defect and Diffusion Forum, 2006, 249, 235-238.	0.4	6
178	Hardness of Nanostructured Al-Zn, Al-Mg and Al-Zn-Mg Alloys Obtained by High-Pressure Torsion. Defect and Diffusion Forum, 2006, 249, 155-160.	0.4	7
179	The Grain Boundary Wetting in the Sn– 25 at% In Alloys. Defect and Diffusion Forum, 2006, 258-260, 491-496.	0.4	3
180	High-Pressure Influence on the Kinetics of Grain Boundary Segregation in the Cu–Bi System. Defect and Diffusion Forum, 2006, 258-260, 390-396.	0.4	0

#	Article	IF	CITATIONS
181	Reconstruction of Brass for Tongues and Shallots from Baroque Organs. Defect and Diffusion Forum, 2006, 258-260, 397-402.	0.4	2
182	Shape of Moving Grain Boundary and its Influence on Grain Boundary Motion in Zinc. Defect and Diffusion Forum, 2006, 249, 183-188.	0.4	0
183	Faceting of Σ3 and Σ9 grain boundaries in Cu–Bi alloys. Acta Materialia, 2005, 53, 247-254.	7.9	28
184	Influence of grain boundary inclination on the grain boundary and triple junction motion in Zn. Materialwissenschaft Und Werkstofftechnik, 2005, 36, 528-532.	0.9	3
185	Faceting of the Σ 3 coincidence tilt boundary in Nb. Journal of Materials Science, 2005, 40, 871-874.	3.7	9
186	The Temperature Influence on the Faceting of Ʃ3 Grain Boundaries in Aluminium. Defect and Diffusion Forum, 2005, 237-240, 603-608.	0.4	7
187	Faceting of Ʃ3 Grain Boundaries in Cu: Three-Dimensional Wulff Diagrams. Defect and Diffusion Forum, 2005, 237-240, 584-592.	0.4	4
188	Grain-boundary melting phase transition in theCuâ^'Bisystem. Physical Review B, 2005, 71, .	3.2	104
189	Formation of Nanostructure during High-Pressure Torsion of Al-Zn, Al-Mg and Al-Zn-Mg Alloys. Defect and Diffusion Forum, 2005, 237-240, 739-744.	0.4	17
190	Faceting and migration of twin grain boundaries in zinc. International Journal of Materials Research, 2005, 96, 161-166.	0.8	23
191	The influence of misorientation deviation on the faceting of Σ3 grain boundaries in aluminium. International Journal of Materials Research, 2005, 96, 216-219.	0.8	11
192	Influence of faceting-roughening on triple-junction migration in zinc. International Journal of Materials Research, 2005, 96, 1147-1151.	0.8	21
193	Pokrovsky-Talapov Critical Behavior and Rough-to-Rough Ridges of theΣ3Coincidence Tilt Boundary in Mo. Physical Review Letters, 2004, 92, 196101.	7.8	17
194	Grain boundary faceting close to the Σ3 coincidence misorientation in copper. International Journal of Materials Research, 2004, 95, 939-944.	0.8	12
195	Grain Boundary Phase Transitions and their Influence on Properties of Polycrystals. Journal of Materials Science, 2004, 12, 147-155.	1.2	87
196	Formation of nanograined structure and decomposition of supersaturated solid solution during high pressure torsion of Al–Zn and Al–Mg alloys. Acta Materialia, 2004, 52, 4469-4478.	7.9	247
197	Grain boundary wetting by a solid phase; microstructural development in a Zn–5 wt% Al alloy. Acta Materialia, 2004, 52, 4537-4545.	7.9	103
198	Grain Boundary Phase Transitions in the Al–Mg System and Their Influence on High-Strain Rate Superplasticity. Defect and Diffusion Forum, 2003, 216-217, 307-312.	0.4	22

#	Article	IF	CITATIONS
199	Influence of the Grain Boundary Phase Transitions on the Diffusion-Related Properties. Defect and Diffusion Forum, 2003, 216-217, 53-64.	0.4	6
200	Diffusion Degradation of Carbon Coatings on Various Metallic Substrates. Defect and Diffusion Forum, 2003, 216-217, 323-330.	0.4	0
201	Grain Boundary Faceting Phase Transition and Thermal Grooving in Cu. Defect and Diffusion Forum, 2003, 216-217, 93-100.	0.4	3
202	Grain boundary phase transitions and phase diagrams. Solid State Sciences, 2001, 3, 1113-1115.	0.7	77
203	Vacuum arc deposition of protective layers on glass and polymer substrates. Thin Solid Films, 2001, 383, 224-226.	1.8	9
204	Faceting and Roughening of the Asymmetric Twin Grain Boundaries in Zinc. Journal of Materials Science, 2001, 9, 275-279.	1.2	17
205	Faceting of Σ3 and Σ9 Grain Boundaries in Copper. Journal of Materials Science, 2001, 9, 287-292.	1.2	75
206	Grain Boundary Grooving as an Indicator of Grain Boundary Phase Transformations. Journal of Materials Science, 2001, 9, 43-53.	1.2	72
207	Grain Boundary Phase Transitions in the Cu-Bi System. Defect and Diffusion Forum, 2001, 194-199, 1343-1348.	0.4	16
208	Ionic Nitriding of Austenitic and Ferritic Steel with the Aid of a High Aperture Hall Current Accelerator. Defect and Diffusion Forum, 2001, 194-199, 1457-1462.	0.4	8
209	Meyer-Neldel Rule for the Kinetic Properties of Grain and Interphase Boundaries. Defect and Diffusion Forum, 2001, 192-193, 15-26.	0.4	8
210	Influence of Grain Boundary Phase Transitions on the Properties of Cu-Bi Polycrystals. Defect and Diffusion Forum, 2001, 188-190, 185-0.	0.4	18
211	Corrosion resistance of the vacuum arc deposited Ti, TiN and TiO2 coatings on large area glass substrates. Surface and Coatings Technology, 2000, 125, 223-228.	4.8	16
212	Corrosion behaviour of the protective and decorative TiN coatings on large area steel strips. Surface and Coatings Technology, 2000, 125, 229-232.	4.8	23
213	Vacuum arc deposition of Ti coatings. Surface and Coatings Technology, 2000, 125, 157-160.	4.8	7
214	Pre-treatment of large area strips with the aid of a high power Hall current accelerator. Surface and Coatings Technology, 2000, 125, 35-39.	4.8	3
215	Decay kinetics of nonequilibrium Al-Si solid solutions. Physical Review B, 2000, 61, 6019-6027.	3.2	7
216	Tie Lines of the Grain Boundary Wetting Phase Transition in the Zn-Rich Part of the Zn-Sn Phase Diagram. Materials Science Forum, 1999, 294-296, 411-414.	0.3	40

#	Article	IF	CITATIONS
217	Kinetics of the Bi Segregation at Grain Boundaries in Polycrystalline Cu. Materials Science Forum, 1999, 294-296, 585-588.	0.3	3
218	Radiotracer Diffusion of Ni and Ag in Ag and Ni Grain Boundaries and Oriented Ag/Ni Interphase Boundaries. Materials Science Forum, 1999, 294-296, 541-544.	0.3	11
219	Masked deposition of decorative coatings on large area glass and plastic sheets. Thin Solid Films, 1999, 351, 204-208.	1.8	15
220	Hall current accelerator for pre-treatment of large area glass sheets. Thin Solid Films, 1999, 351, 190-193.	1.8	9
221	Thermodynamic aspects of the grain boundary segregation in Cu(Bi) alloys. Acta Materialia, 1999, 47, 4041-4046.	7.9	105
222	Excess Volume of the Solid/Liquid Interface in Fe-6 at.%Si Bicrystals Wetted by Liquid Zinc. Journal of Materials Science, 1998, 6, 179-186.	1.2	9
223	Stable and metastable phases in the vacuum arc deposited Co thin films. Thin Solid Films, 1998, 319, 124-127.	1.8	15
224	Vacuum arc deposition of Ni-Ti gradient coatings. Surface and Coatings Technology, 1998, 100-101, 316-319.	4.8	3
225	The Effect of Pressure on Grain Boundary Wetting, Segregation and Diffusion. Defect and Diffusion Forum, 1998, 156, 163-174.	0.4	6
226	Grain Boundary Segregation in the Cu-Bi System. Defect and Diffusion Forum, 1998, 156, 135-146.	0.4	66
227	The Grain Structure of Vacuum Arc Deposited Co Thin Films. Materials Science Forum, 1998, 294-296, 787-790.	0.3	0
228	Normal and Abnormal Grain Growth in Tungsten Polycrystals. Materials Science Forum, 1998, 294-296, 533-536.	0.3	1
229	Effect of Temperature and Pressure on Grain Boundary Segregation and Wetting. Defect and Diffusion Forum, 1997, 143-147, 1407-1412.	0.4	5
230	Vacuum Arc Deposited Mo Layers: Grain Size and Roughness. Defect and Diffusion Forum, 1997, 143-147, 1637-1644.	0.4	2
231	Grain Boundary Wetting Phase Transition in the Mo-Ni System. Defect and Diffusion Forum, 1997, 143-147, 1517-1522.	0.4	10
232	Mechanism of Diffusion Induced Recrystallization in Single Crystals of Copper. Defect and Diffusion Forum, 1997, 143-147, 1589-1594.	0.4	4
233	Solute drag and wetting of a grain boundary. Philosophical Magazine Letters, 1997, 76, 133-138.	1.2	13
234	Pressure influence on the grain boundary wetting phase transition in Feî—,Si alloys. Acta Materialia, 1997, 45, 1931-1940.	7.9	71

#	Article	IF	CITATIONS
235	Temperature dependence of the grain boundary segregation of Bi in Cu polycrystals. Scripta Materialia, 1997, 37, 729-735.	5.2	70
236	Morphology of Mo particles and their incorporation into the growing film during vacuum arc deposition. Nuclear Instruments & Methods in Physics Research B, 1997, 122, 594-597.	1.4	4
237	The Solidus Line of the Cu-Bi Phase Diagram. Journal of Phase Equilibria and Diffusion, 1997, 18, 128-135.	0.3	72
238	Abnormal grain growth in Al of different purity. Materials & Design, 1997, 18, 293-295.	5.1	7
239	Hypereutectic Al-Si based alloys with a thixotropic microstructure produced by ultrasonic treatment. Materials & Design, 1997, 18, 323-326.	5.1	73
240	Vacuum arc deposition as a complementary technology to laser processing. Applied Surface Science, 1997, 109-110, 437-441.	6.1	6
241	Lines of Grain Boundary Phase Transitions in Bulk Phase Diagrams. Materials Science Forum, 1996, 207-209, 59-68.	0.3	29
242	Diffusion Induced Stresses as a Driving Force for the Instability of a Solid/Liquid Interface. Defect and Diffusion Forum, 1996, 129-130, 229-242.	0.4	1
243	Grain Boundary Wetting Phase Transitions on the Al-Sn and Al-Sn-Pb Systems. Materials Science Forum, 1996, 207-209, 437-440.	0.3	15
244	The Onset of Abnormal Grain Growth in Al-Ga Polycrystals. Materials Science Forum, 1996, 207-209, 557-560.	0.3	2
245	Liquid film migration in a Mo(Ni) bicrystal. Philosophical Magazine Letters, 1996, 73, 187-194.	1.2	17
246	Vacuum arc deposition of Mo films. Journal of Vacuum Science and Technology A: Vacuum, Surfaces and Films, 1996, 14, 3252-3255.	2.1	15
247	Diffusion induced recrystallization in single crystals of copper. Physica Status Solidi A, 1995, 150, 705-713.	1.7	2
248	Preparation of Feî—,Si single crystals and bicrystals for diffusion experiments by the electron-beam floating zone technique. Journal of Crystal Growth, 1995, 151, 180-186.	1.5	35
249	Acceleration of grain boundary motion in Al by small additions of Ga. Philosophical Magazine Letters, 1995, 72, 361-368.	1.2	68
250	The influence of an ordering transition on the interdiffusion in Au-Cu alloys. Acta Metallurgica Et Materialia, 1995, 43, 1817-1823.	1.8	4
251	The influence of an ordering transition on the interdiffusion in Fe-Si alloys. Acta Metallurgica Et Materialia, 1995, 43, 3075-3083.	1.8	31
252	Grain Boundary Zinc Penetration in Fe-Si Alloys: Premelting Phase Transition on the Grain Boundaries. Materials Science Forum, 1993, 126-128, 391-394.	0.3	5

#	Article	IF	CITATIONS
253	The wetting transition in high and low energy grain boundaries in the Cu(In) system. Acta Metallurgica Et Materialia, 1992, 40, 939-945.	1.8	74
254	Premelting transition on 38°ã€^100〉 tilt grain boundaries in (Fe-10 at.% Si)-Zn alloys. Acta Metallurgica Et Materialia, 1992, 40, 795-801.	1.8	64
255	High temperature DIGM in an Fe-5 at.% Al bicrystal during Zn diffusion. Scripta Metallurgica Et Materialia, 1992, 26, 901-906.	1.0	6
256	Wetting phenomena on external and internal interfaces in solids: common features and peculiarities. Surface Science, 1991, 251-252, 674-679.	1.9	1
257	The zinc penetration along tilt grain boundary 38° [100] in Fe-12at.%Si alloy near ordering A2 - B2 in the bulk. Scripta Metallurgica Et Materialia, 1991, 25, 1441-1446.	1.0	2
258	Wetting and premelting phase transitions in 38° [100] tilt grain boundary in (Fe-12 at.% Si)-Zn alloy in the vicinity of the A2-B2 bulk ordering in Fe-12 at.% Si alloy. Acta Metallurgica Et Materialia, 1991, 39, 3091-3098.	1.8	67
259	Penetration of tin and zinc along tilt grain boundaries 43° [100] in Fe-5 at.% Si alloy: Premelting phase transition?. Acta Metallurgica Et Materialia, 1991, 39, 627-639.	1.8	74
260	GRAIN BOUNDARIES: PHASE TRANSITIONS AND CRITICAL PHENOMENA. International Journal of Modern Physics B, 1991, 05, 2989-3028.	2.0	68
261	Diffusion of indium along [001] Snî—,Ge interphase boundaries: Prewetting phase transition and critical phenomena. Journal of the Less Common Metals, 1990, 159, 43-52.	0.8	10
262	Diffusion of indium along [001] twist boundaries in tin: Concentrational β-γ′ phase transition on grain boundaries. Journal of the Less Common Metals, 1990, 158, 23-33.	0.8	9
263	Phase transitions at grain boundaries in the presence of impurities. Acta Metallurgica, 1989, 37, 1995-1998.	2.1	17
264	Effect of the subsidiary misorientation components on the "special grain boundary-general boundary― transformation in the vicinity of the coincidence misorientation of Σ17 in tin. Acta Metallurgica, 1989, 37, 2855-2860.	2.1	16
265	Transformation of â~'17 special tilt boundaries to general boundaries in tin. Acta Metallurgica, 1988, 36, 1573-1583.	2.1	71
266	Regions of existence of special and non-special grain boundaries. Acta Metallurgica, 1985, 33, 1735-1749.	2.1	163
267	The effect of crystallographic parameters of interphase boundaries on their surface tension and parameters of the boundary diffusion. Acta Metallurgica, 1984, 32, 1355-1364.	2.1	40
268	The effect of pressure on migration of ã€^001〉 tilt grain boundaries in tin bicrystals. Scripta Metallurgica, 1984, 18, 207-211.	1.2	68
269	The influence of pressure on indium diffusion along single tin-germanium interphase boundaries. Scripta Metallurgica, 1983, 17, 275-279.	1.2	37
270	Indium diffusion along interphase twist boundaries Snî—,Ge. Scripta Metallurgica, 1981, 15, 1197-1200.	1.2	18

#	Article	IF	CITATIONS
271	Enhanced Ductility in Ultrafine-Grained Al Alloys Produced by SPD Techniques. Materials Science Forum, 0, 633-634, 321-332.	0.3	20
272	The Effect of Grain Boundary Sliding and Strain Rate Sensitivity on the Ductility of Ultrafine-Grained Materials. Materials Science Forum, 0, 667-669, 677-682.	0.3	17
273	Grain Boundary Segregation and Amount of Bulk Carbides in Severely Deformed Fe–C Alloys. Defect and Diffusion Forum, 0, 309-310, 51-62.	0.4	6
274	Pseudopartial Grain Boundary Wetting: Key to the Thin Intergranular Layers. Defect and Diffusion Forum, 0, 333, 175-192.	0.4	25
275	Diffusion and Phase Transitions Accelerated by Severe Plastic Deformation. , 0, 5, 95-108.		11